

Fault damage zone at subsurface: A case study using 3D seismic attributes and a clay model analog for the Anadarko Basin, Oklahoma

Zonghu Liao¹, Hui Liu², Zheng Jiang³, Kurt J. Marfurt⁴, and Ze'ev Reches⁴

Abstract

Using 3D seismic attributes and the support of a clay model that served as an analog, we mapped and analyzed a 32 km (20 mi) long, north–south-striking, right-lateral fault in the Woodford Shale, Anadarko Basin, Oklahoma, USA. Volumetric coherence, dip azimuth, and curvature delineated an approximately 1.5 km (approximately 5000 ft) wide damage zone with multiple secondary faults, folds, and flexures. The clay analog enabled us to identify these features as belonging to a complex transpressional Riedel structure. We also suggest that the damage zone contains dense subseismic fractures associated with multiscale faulting and secondary folding that may correspond to highly permeable features within the Woodford Shale.

Introduction

Fractures, fracture clusters, and tensile zones are typically below seismic resolution (Munthe et al., 1993; Fossen and Hesthammer, 2000; Al-Dossary and Marfurt, 2006); thus, their distribution is sometimes indirectly deduced from their location with regard to large-scale structures (Lisle, 1994; Chester et al., 2004) or 3D seismic attributes (Chopra, 2010). Lisle (1994) shows that the strain associated with the local curvature of large-scale folds may lead to the local development of fracture networks. Roberts (2001) uses this concept to estimate the fracture distribution from curvature computed along seismic horizon maps, and Hart et al. (2002) apply it to the Pennsylvanian Paradox carbonates in New Mexico. Many authors have attempted to derive geologically based approaches to predict fracture intensity; for instance, McLennan et al. (2009) combine outcrop observations from Hennings et al. (2000) with multivariate analysis of the structural properties of the Oil Mountain anticline, near Casper, Wyoming, to create predictive fracture models. These studies indicate that we can relate fracture intensity to bedding curvature and its gradient in which curvature provides a direct measure of accumulated strain. However, natural fractures may also be related to regional deformation (Kelley and Clinton, 1960; Reches, 1976), diagenesis (Ellis et al., 2012), and unloading (Faulkner et al., 2010), with no clear relations to local curvature or strain. Some recent studies that correlate fracture distribution with 3D seismic attributes

have focused on anticlinal structures, in which the fracture intensity is related to curvature, change of curvature, and local strain (Gao, 2013; Wilson et al., 2015).

To investigate the fracture distribution at the subsurface, we interpret and analyze the damage zone of a large strike-slip fault, following the well-documented observation that damage zones are dissected by multiple faults, and fractures, and generate local folding (Harding, 1974; Dieterich and Smith, 2009; Faulkner et al., 2010). Faults and fault-related folds control the subsidiary fractures that in turn may control the migration, accumulation, or leakage of hydrocarbons in sedimentary basins (Aydin 2000; Faulkner et al., 2010). However, we should always remember that, within a short distance (of the order of tens of meters) from the fault zone, the locus, abundance, openness, and other fracture attributes likely to affect the fluid flow may significantly change even in the same structural position relative to the larger structure (Ellis et al., 2012).

This study focuses on the Woodford Shale, an important hydrocarbon source rock of Upper Devonian to Lower Mississippian age (Anadarko Basin, central-western Oklahoma; Figure 1a) that has produced dry gas and oil from an approximately 30–50 m thick reservoir since 2004 (Comer, 1991; Lambert, 1993; Cardott, 2012). The Anadarko Basin is dominated by large transpressional tectonism.

Hydraulic fracturing, along with horizontal drilling, has revolutionized the development of unconventional

¹China University of Petroleum, State Key Laboratory of Petroleum Resources and Prospecting, Beijing, China and University of Oklahoma, School of Geology and Geophysics, Norman, Oklahoma, USA. E-mail: zonghuliao@163.com.

²China University of Petroleum, State Key Laboratory of Petroleum Resources and Prospecting, Beijing, China. E-mail: liuhuie_mail@163.com.

³Peking University, College of Engineering, Beijing, China. E-mail: zheng.jiang@pku.edu.cn.

⁴University of Oklahoma, School of Geology and Geophysics, Norman, Oklahoma, USA. E-mail: kmarfurt@ou.edu; reches@ou.edu.

Manuscript received by the Editor 22 February 2016; revised manuscript received 17 September 2016; published online 08 February 2017. This paper appears in *Interpretation*, Vol. 5, No. 2 (May 2017); p. T143–T150, 6 FIGS.

<http://dx.doi.org/10.1190/INT-2016-0033.1>. © 2017 Society of Exploration Geophysicists and American Association of Petroleum Geologists. All rights reserved.

reservoirs (Abousleiman et al., 2007; Waters et al., 2009; Badra, 2011). The artificial fracturing is likely to reactivate natural fractures and open weak cemented zones (Buseti, 2009). Natural fracture systems can improve production efficiency (Gidley, 1989); however, such fractures can also connect reservoirs with neighboring aquifers. Therefore, mapping the distribution of natural fractures plays an important role in designing the depth and orientation of the horizontal wells, as well as the

location and extent of completion strategies (Gale et al., 2007).

We analyze a complex fault/fracture system in the Woodford Shale seen on selected volumetric seismic attributes (Marfurt and Rich, 2010) with the support of a clay analog model (Reches, 1988; McClay and Bonora, 2001), similarly to Staples (2011) who uses clay models to help interpret complex fracturing inferred from a 3D reflection seismic survey acquired over the Woodford play in northeast Oklahoma. Mechanical and experimental analysis provides laboratory analogs from which the development of subseismic features can be understood (Naylor et al., 1986; Reches, 1988).

We begin with a review of the geology of the study area and describe some of the geometric features exhibited in a strike-slip system. Next, we describe our clay model experiment and we compute volumetric seismic attributes from a 3D megamerger seismic reflection survey (Figure 1a). Finally, we couple the structural features observed on the seismic volumes to those of the clay model to predict the internal structures of the damage zone of the strike-slip fault.

The El Reno fault zone, central-western Oklahoma

The selected study area is in the Anadarko Basin, Oklahoma, USA (Figure 1a), which is deformed during the late Mississippian by structural inversion of the southern Oklahoma aulacogen. The structural development of the basin is dominated by complex transpressional tectonism, as a combined influence of the Wichita thrust system and the subsequent Arbuckle thrust system. The strike-slip faulting in the southwestern Arbuckle Mountains generated the strike-slip faulting in the Anadarko Basin (Perry, 1989).

Our focus is the Woodford Shale unit (Upper Devonian to Lower Mississippian), which includes important petroleum source rock within the United States Mid-continent. This unit was deposited under anoxic conditions in the Anadarko Basin during the Kaskaskian marine transgression (Johnson, 1988; Lambert, 1993; Paxton et al., 2006; Cardott, 2012). The Woodford Shale is a laminated, organic-rich unit with alternating brittle and ductile layers (Slatt et al., 2010). The fractures in the brittle layers (rich in quartz and calcite) are normal to the bedding and often filled with bitumen (Bernal et al., 2012). The ductile layers (rich in clay and organic carbon) are typically deformed by shear flow (Reches, 1987).

In the study area, the two-way traveltime (TWT) map of the top of the Woodford Shale (Figure 1b) gently dips (<2°) toward the southwest, with the paleoshoreline located in the northeast and the depocenter in the southeast (Gupta, 2012). Two major fault trends are approximately perpendicular to each other and can be observed on the TWT structural map. Our study focuses on the El Reno fault (ERF), a significant north-south-striking structure in the eastern part of the study area (Figure 1b). The vertical seismic section perpendicular to the ERF (Figure 1c) indicates that, at the level of the

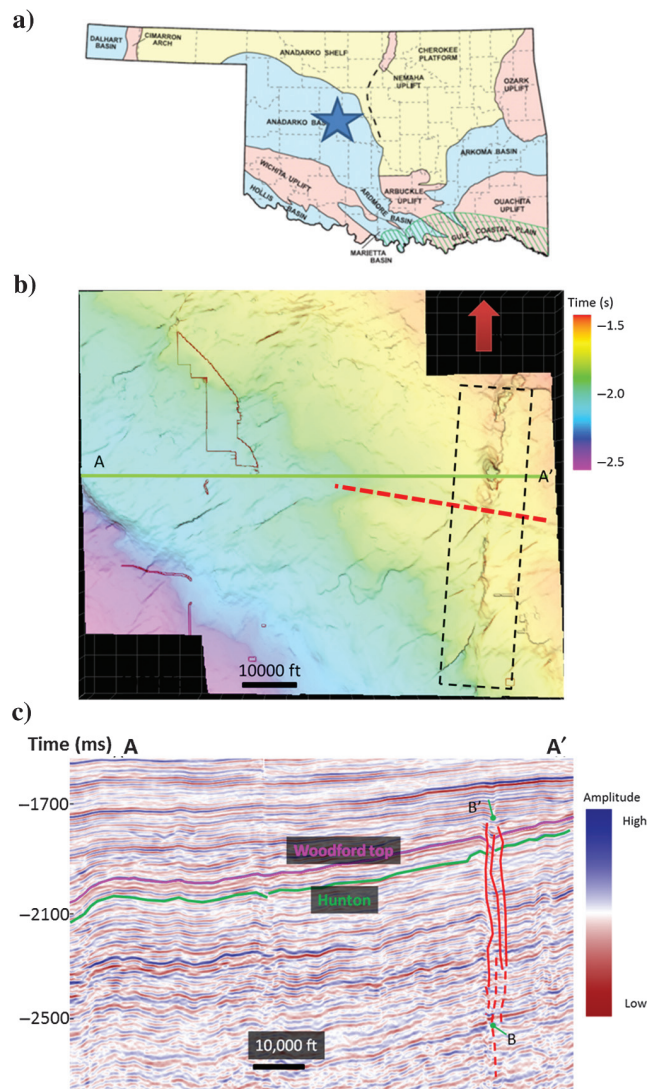


Figure 1. (a) General location of the study area (blue star) in the Anadarko Basin, Oklahoma (base map modified from Northcutt and Campbell, 1995). (b) TWT map of the top of the Woodford Shale showing gentle dipping (<2°) toward the southwest. The structural time map reveals structural elements, including the north-south ERF zone within the black dashed rectangle, and the normal fault (in the dotted red line) perpendicular to the ERF. (c) Seismic amplitude vertical cross section along AA' (b). The three vertical red lines, marked BB', are the interpreted major segments of the ERF zone through the cross section. The pink and green horizons indicate the top of the Woodford Shale and the top of Hunton Formation, respectively.

Woodford Shale, the ERF displaces rotated layers with a throw exceeding approximately 80 m in places.

Several structural features suggest that the ERF is a strike-slip system. First, it is a vertical fault zone that comprises several subparallel, vertical segments (Figure 1c), typical of strike-slip faults (Harding, 1974, 1985; Christie-Blick and Biddle, 1985). Second, it has relatively small throws (up to 80 m) compared to its large horizontal (32 km, Figure 1b) and vertical (at least 500 ms, Figure 1c) extents, which strongly suggests that the predominant displacement is subhorizontal. Finally, the sense of vertical throw varies among different stratigraphic levels. As an example in Figure 1c, the west side is downthrown at location B, whereas the east block is downthrown at location B'.

Strike-slip faulting in clay experiments

Clay cake models have been widely used to study strike-slip faulting (Cloos, 1932; Wilcox et al., 1973; Freund, 1974; Naylor et al., 1986; Reches, 1988; McClay and Bonora, 2001). In a typical experiment, a soft layer (wet clay or loose sand) overlies a two-block rigid layer that represents the basement and the separation between the two blocks emulates a strike-slip fault (Figure 2a). The soft layer undergoes simple shear parallel to the basement fault, and this shear leads to the development of several distinct secondary structures (Naylor et al., 1986): (1) Riedel shears (R), small strike-slip fault trending approximately 15° relative to the basement fault, with slip direction subparallel to the basement fault; (2) conjugate Riedel shears (R') that strike at approximately 75° – 90° to the basement fault, only occasionally observed; (3) short-lived splay faults near the tips of the Riedel shears striking at more than 17° to the basement fault; and (4) P-shears that typically appear after an advanced stage of deformation, and connect discontinuous Riedel shears. Additional associated structures are folds and thrust faults oriented approximately 45° with respect to the basement fault, and secondary normal faults oriented approximately 135° with respect to the main fault (Reches, 1988).

We used clay models as a guide to interpret the evolution of a strike-slip fault and its associated structures, and we compared them with the structure of the ERF as revealed in the 3D seismic attribute analysis; however, we did not consider the experiment as a scale model. In our experiment, the clay density was 1.22 g/cm^3 (76.2 lb/f^3), and the model was nearly 15 cm (length) \times 15 cm (width) \times 5 cm (thickness). The clay cake was placed on the top of two wooden plates that moved laterally with respect to each other at a constant

right-lateral motion of 0.058 cm/s to a total slip distance of approximately 1.4 cm after 24 min (Figure 2b and 2c). The boundary conditions in the model construction correspond to a strike-slip fault created by lateral motion along the reactivated basement fault. The clay deformation was recorded on photographs taken every 30 s. Our experiment generated fault patterns similar to the classical case (Naylor et al., 1986) with dominance of secondary Riedel shears, splay faults, and P-shears (Figure 3a).

Seismic attribute analysis

The 3D seismic reflection data covering the study area comprise nine narrow azimuth surveys acquired in central Oklahoma between 1994 and 2011 to image the Red Fork sandstones of Middle Pennsylvanian age. In 2012, the nine surveys were reprocessed together for prestack time migration using a single datum and a common bin size ($33.5 \times 33.5 \text{ m}$ or $110 \times 110 \text{ ft}$). At the top of the Woodford Shale, deeper than the original seismic acquisition target, the frequencies range between 10 and 60 Hz, and the fold coverage varies from 15 to 60.

We computed volumetric seismic attributes (coherence, curvature, and dip azimuth) following Marfurt and Rich (2010). Next, we extracted the attribute values along the TWT map of the top of the Woodford Shale to reveal the deformation associated with the ERF.

Chopra and Marfurt (2007) define “coherence” as the energy of the coherent part of seismic traces divided by

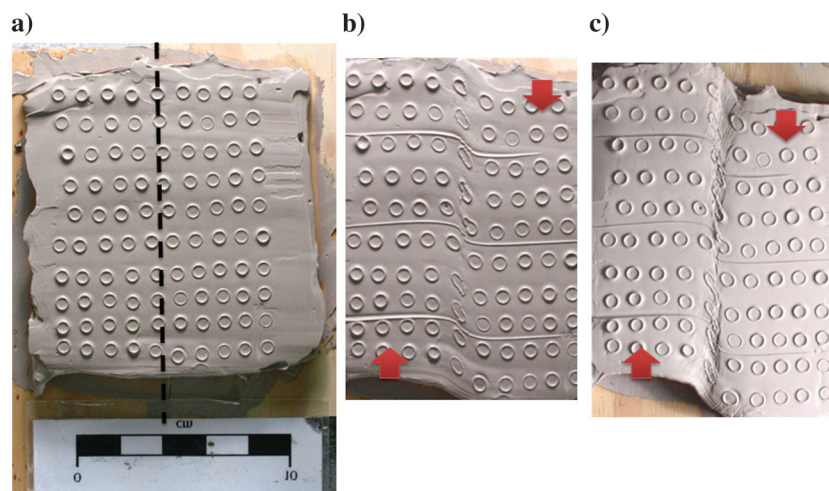


Figure 2. (a) Map view of the clay experiment to model the overburden response to a right-lateral strike-slip fault in a rigid basement indicated by the black dashed line. Circles on the undeformed model provide a means of mapping movement and strain. (b) Photograph taken after 12 min demonstrating the accumulation of strain about the “basement” fault and the beginning of the formation of Riedel (R) shear faults in the ductile overburden. (c) Photograph after 24 min (end of the experiment) showing fault Riedel shears (black lines in Figure 3a), splay shears (green lines in Figure 3a), and P-shears (red lines in Figure 3a) formed on the top of the deformed clay (overburden). The red arrows in (b and c) present the moving direction of the basement fault blocks.

the average acoustic energy of the input seismic traces. The energy-ratio coherence algorithm we applied is similar to the one described by Gerztenkorn and Marfurt (1999), and it is sensitive to lateral changes in waveform, but not in amplitude.

The TWT structural map of the Woodford Shale in the ERF area, corendered with the 3D seismic coherence (Figure 3b), reveals the following features: (1) a major north–south-trending structure interrupted by several discontinuities that we refer to as the ERF, and locally characterized by red patches of low coherence, and (2) northeast–southwest-trending lineaments of medium coherence striking between 15° and 60° relatively to the ERF. Compared with the results of the clay experiment (Figure 3a), we may interpret the observed attribute features (Figure 3c) as follows: (1) The lineaments striking at 15°–30° are the major Riedel (R) shears (black lines), (2) the lineaments striking at 60° are splay faults (green lines), and (3) the red-colored patches along the ERF are P-shears (red lines). Conjugate Riedel shear (R') was not observed.

Next, we examined the patterns on the corendered dip-magnitude and dip-azimuth attribute volumes

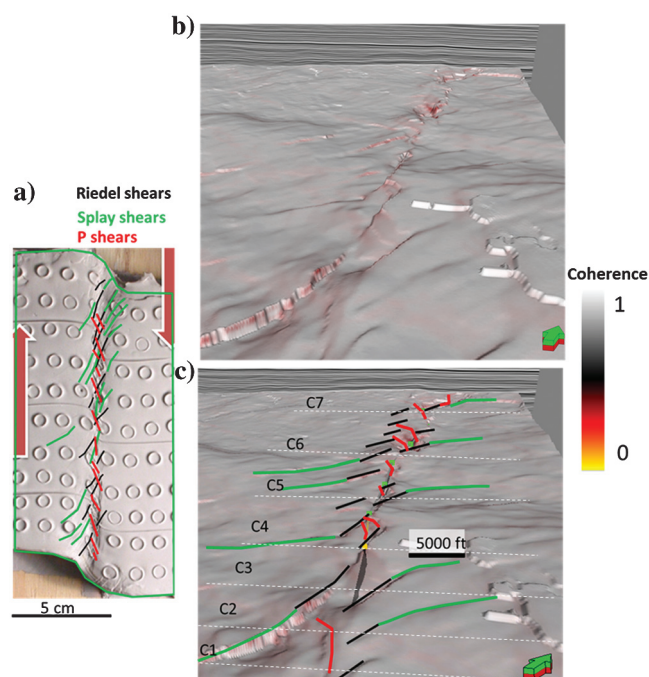


Figure 3. (a) A 3D view of coherence corendered with seismic amplitude along the top of the Woodford Shale and (b) its interpretation. The black lines indicate potential Riedel faults (R); the green lines are interpreted as splay faults, and the red lines are interpreted as P-shears. Indexes C1–C7 indicate corridors for coherence extraction perpendicular to the fault displayed in Figure 6. (c) A photograph from the laboratory experiment taken after 24 min. The fault interpretation on the model conforms to the structural interpretation of the top of the Woodford Shale. The connected points are interpreted fault planes.

along the top of the Woodford Shale (Figure 4). The dip magnitude attribute measures the magnitude of the local dip, whereas the dip azimuth indicates the direction of maximum inclination perpendicular to the strike (Chopra and Marfurt, 2007). The map of the ERF area displays three characteristic features: (1) layers dipping to 180° and 360°, marked by patches of yellow and blue, (2) northeast–southwest-trending lineaments in red-orange (dipping southeast), cyan (dipping northwest), and darker blue (dipping southeast), and (3) northwest–southeast-oriented bands along the ERF in pink-red (dipping eastward), and wide bands across the study area in green-yellow (dipping southwest). We interpret these features as follows: (1) different bedding dip directions, with yellow representing southwest-dipping beds and blue representing north-dipping beds, (2) the northeast–southwest-trending lineaments fit the predicted orientation of R-shears with respect to the main ERF trend, and (3) the pink-red areas are ERF-related secondary anticlinal folds (ridges) reflecting ondulation of the fault plane.

Following Chopra and Marfurt (2007), we also corendered the most positive (K1) and the most negative (K2) principal curvature volumes to identify folds and flexures related to the ERF and the associated Riedel structure (Figure 5). Curvatures are computed as the second derivative of the surface. We interpreted the local most

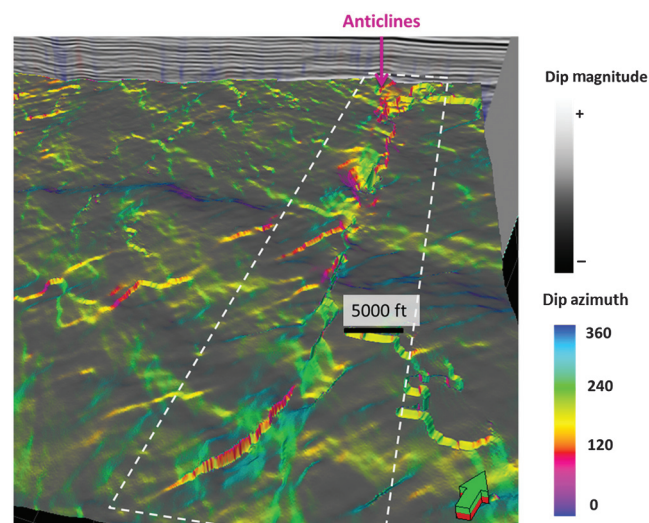


Figure 4. Dip-magnitude map of the top of the Woodford Shale corendered with dip azimuth. The area of the pink color reveals potential fracture zones with compressed folds (ridges). The black/gray color shows the low dip magnitude area on the map. The bright part of the area presents higher dip magnitude. Based on the color palette of dip azimuth, relatively high magnitude dips dipping toward: north (0° or 360°) is blue; south (180°) is yellow; green indicates high-magnitude dips dipping toward the southwest (approximately 240°); and cyan indicates high-magnitude dips dipping toward the northwest (approximately 300°).

positive structures (red) as “ridges” and the most negative structures (blue) as “valleys.”

Discussion: Fault damage zones

Our goal is to combine the laboratory-scale clay model of a strike-slip fault and the field scale analysis of the subsurface strike-slip fault on the 3D reflection seismic data to map the first-order structural features at both scales as a tool to estimate the ERF in situ damage zone. We anticipate that the damage zones are with the highest fracture intensity.

We first examine the clay model. The experiment simulating the movement of a strike-slip fault in a rigid basement (Figure 2) reveals localized deformation within the overlying soft layer. The simple shear generated a zone of secondary, small structures, including Riedel shears, and normal faults; none of these structures is parallel to the basement fault. In the following stage of continuous slip accumulation along the basement fault, some of the secondary faults merge and coalesce to form a continuous, large fault zone that cuts across the entire soft layer parallel to the basement fault. This strike-slip fault is associated with a complex fault system composed of multiple segments and wide damage zone that reflect its prolonged evolution (Naylor et al., 1986).

At seismic scale, the ERF and the associated structures can be observed at the top of the Woodford Shale on coherence (Figure 3), dip azimuth (Figure 4), and curvature (Figure 5) maps. These seismic attributes reveal a complex system of secondary structures that is most intense close to the primary fault plane. The fault features resemble the structures generated in our clay model; therefore, we suggest that the ERF followed an evolutionary path similar to the one we reproduced in the laboratory. Therefore, we assume that the ERF segmented surface led to a heterogeneous stress field with advanced deformation and intense fracturing of the damage zone similar to the laboratory experiment. However, the fault mechanism could be much more complex because lithology and diagenesis are expected to play a significant role in controlling fracture distribution, but these variables have not been accounted for in our experimental model.

We evaluate the damage zone thickness by measuring coherence values along transects across the main fault (Figure 3c) and plotting them on a graph (Figure 6). A zone of low coherence values occupies a zone of approximately 1500 m (5000 ft) centered on the ERF (Figure 6). We regard this zone of low coherence as an area of high damage due to dense secondary faults and fractures. It is expected that the extension associated with layer bends (Reches and Johnson, 1978) will correlate with the local, higher intensity of natural fractures (Stearns, 1978; Guo et al., 2010; Staples et al., 2011).

One of the main limiting factors in our ERF interpretation is the existence of similar-scale structures due to a major faults trend perpendicular to the ERF, possibly

related to a much larger deformation system. The uncertainty could be overcome by larger seismic investigations covering a larger area in the future. In addition, there is a lack of information on the subsurface fracture intensity correlated with the ERF and its associated structures. In the future, image logs in this study area might provide consistent data to support our subsurface damage zone analysis. With a better understanding of the damage zone at the subsurface and how the frac-

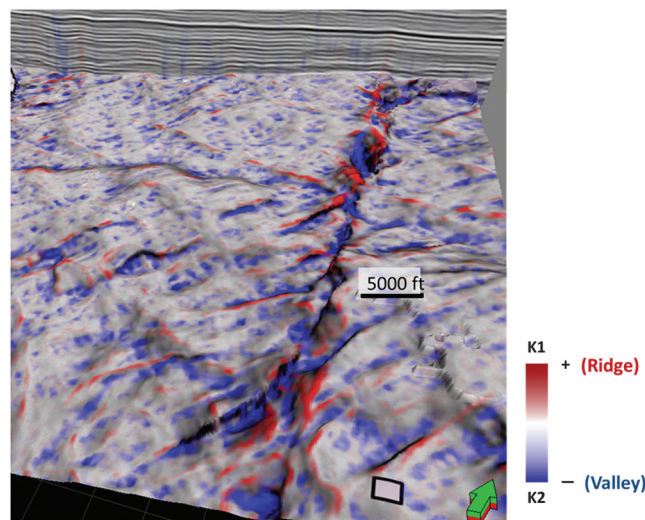


Figure 5. Curvatures of most positive (K1) and most negative (K2) on the top of the Woodford Shale. The K1 and K2 are normal curvatures measured in planes perpendicular to each other on the surface, representing the maximum and minimum curvature. Areas with strong curvature (brighter red indicate ridges and blue valleys) correspond to strong flexures, folds, and possibly a high density of fractures.

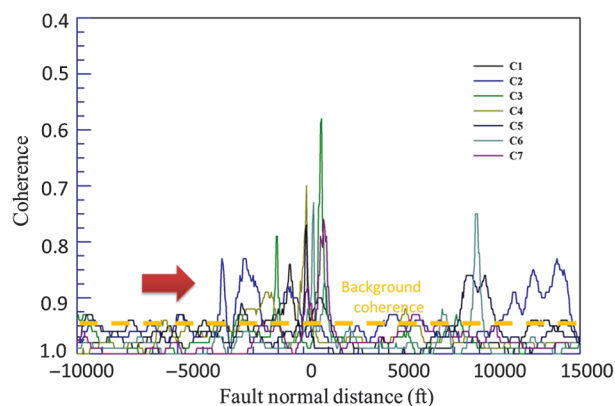


Figure 6. Illustration of the damage zone from the coherence slices perpendicular to the north-south strike-slip fault. Their locations are shown by the indexes C1-C7 in Figure 3c for coherence extraction. The zone (red arrow) of low coherence values indicates the damage zone. The anomalously high values of coherency in the right side might be related to adjacent discontinuities, hence revealing a potential fault zone.

ture density correlates to the fault damage zone, the seismic attributes could provide important clues to the characterization of the fracture networks associated to strike slip faults for well placement and production optimization.

Conclusions

Our clay experiment confirmed that strike-slip faults begin with the development of Riedel shears, followed by splay faults, and finally by P-shears. These features served as the major criteria for proxies to characterize the El Reno strike-slip fault that crosses the Woodford Shale in central-western Oklahoma on three seismic attributes (coherence, dip azimuth, and curvature). The curvature map along the top of the Woodford Shale has previously been presented as an effective indicator of anticlinal folds (ridges) with expected high fracture intensity based on observations from clay experiments.

Whereas normal and reverse faults are relatively simple to recognize on seismic amplitude and attribute data, strike-slip faults are challenging because the horizon correlation across the fault is not straightforward, especially where the horizontal slip is large. We found that combining clay models and seismic attributes helps to characterize a subsurface strike-slip fault system and to infer the details of its damage zone for well placement and reservoir characterization purposes.

Acknowledgments

The authors would like to thank D. Astratti, B. Krantz, and two other anonymous reviewers for their helpful comments; D. Paul for their discussions; N. Gupta for providing data sets and seismic attributes; CGG for providing a license to their 3D seismic data; the sponsors of the Attribute Assisted Seismic Processing and Interpretation (AASPI), University of Oklahoma; and Schlumberger for providing the interpretation platform Petrel. Z. Liao is particularly grateful to G. Randy Keller, director of the Oklahoma Geological Survey, for his support. Additional support funding was provided by the Science Foundation of China University of Petroleum, Beijing (no. 2462014YJRC013) and the National Natural Science Foundation of China (no. 41604036, and the major projects no. U1663203).

References

- Abousleiman, Y., M. Tran, S. Hoang, C. Bobko, A. Ortega, and F.-J. Ulm, 2007, Geomechanics field and laboratory characterization of Woodford Shale: The next gas play: Presented at the SPE Annual Technical Conference and Exhibition, SPE, doi: [10.2118/110120-MS](https://doi.org/10.2118/110120-MS).
- Al-Dossary, S., and K. J. Marfurt, 2006, 3D volumetric multi-spectral estimates of reflector curvature and rotation: *Geophysics*, **71**, no. 5, P41–P51, doi: [10.1190/1.2242449](https://doi.org/10.1190/1.2242449).
- Aydin, A., 2000, Fractures, faults, and hydrocarbon entrapment, migration and flow: *Marine and Petroleum Geology*, **17**, 797–814, doi: [10.1016/S0264-8172\(00\)00020-9](https://doi.org/10.1016/S0264-8172(00)00020-9).
- Badra, H., 2011, Field characterization and analog modeling of natural fractures in the Woodford Shale, southeast Oklahoma: Ph.D. thesis, University of Oklahoma.
- Bernal, A. S., L. C. Mayorga, A. G. Prada, and R. M. Slatt, 2012, Geological characterization of the Woodford Shale, McAlester Cemetery quarry, Oklahoma: *Shale Shaker*, **63**, 202–212.
- Busetti, S., 2009, Fracturing in layered reservoir rocks: Ph.D. thesis, University of Oklahoma.
- Cardott, B. J., 2012, Thermal maturity of Woodford Shale gas and oil plays, Oklahoma, USA: *International Journal of Coal Geology*, **103**, 109–119, doi: [10.1016/j.coal.2012.06.004](https://doi.org/10.1016/j.coal.2012.06.004).
- Chester, F. M., J. S. Chester, D. L. Kirschner, S. E. Schulz, and J. P. Evans, 2004, Structure of large-displacement, strike-slip fault zones in the brittle continental crust, *in* G. D. Karner, B. Taylor, N. W. Driscoll, and D. L. Kohlstedt, eds., *Rheology and deformation in the lithosphere at continental margins*: Columbia University Press, 223–260.
- Chopra, S., 2010, Interpreting fractures through 3-D seismic discontinuity attributes and their visualization: *CSEG Recorder Online*, **34**, <http://csegrecorder.com/articles/view/interpreting-fractures-through-3d-seismic-discontinuity-attributes>, accessed 20 March 2016.
- Chopra, S., and K. J. Marfurt, 2007, Seismic attributes for prospect identification and reservoir characterization: SEG, *Geophysical Developments Series 11*.
- Christie-Blick, N., and K. T. Biddle, 1985, Deformation and basin formation along strike-slip faults, *in* K. T. Biddle, and N. Christie-Blick, eds., *Strike-slip deformation, basin formation, and sedimentation*: SEPM Special Publication 37, 1–34.
- Cloos, E., 1932, “Feather joints” as indicators of the direction of movements on faults, thrusts, joints and magmatic contacts: *Proceedings of the National Academy of Sciences of the United States of America*, **18**, 387–395.
- Comer, J. B., 1991, Potential for producing oil and gas from the Woodford Shale (Devonian-Mississippian) in the southern mid-continent, USA: Presented at the AAPG Annual Convention and Exhibition.
- Dieterich, J. H., and D. E. Smith, 2009, Nonplanar faults: Mechanics of slip and off-fault damage, *in* Y. Ben-Zion, and C. Sammis, eds., *Mechanics, structure and evolution of fault zones*: *Pageoph Topical Volumes 166*, 1799–1815.
- Ellis, M. A., S. E. Laubach, P. Eichhubl, J. E. Olson, and P. Hargrove, 2012, Fracture development and diagenesis of Torridon Group Applecross Formation, near An Teallach, NW Scotland: Millennia of brittle deformation resilience: *Journal of the Geological Society, London*, **169**, 297–310, doi: [10.1144/0016-76492011-086](https://doi.org/10.1144/0016-76492011-086).
- Faulkner, D. R., C. A.-L. Jackson, R. J. Lunn, R. W. Schlichte, Z. K. Shipton, C. A. J. Wibberley, and M. O. Withjack, 2010, A review of recent developments concerning the structure, mechanics and fluid flow properties of

- fault zones: *Journal of Structural Geology*, **32**, 1557–1575, doi: [10.1016/j.jsg.2010.06.009](https://doi.org/10.1016/j.jsg.2010.06.009).
- Fossen, H., and J. Hesthammer, 2000, Possible absence of small faults in the Gullfaks Field, northern North Sea: Implications for downscaling of faults in some porous sandstones: *Journal of Structural Geology*, **22**, 851–863, doi: [10.1016/S0191-8141\(00\)00013-4](https://doi.org/10.1016/S0191-8141(00)00013-4).
- Freund, R., 1974, Kinematics of transform and transcurrent faults: *Tectonophysics*, **21**, 93–134, doi: [10.1016/0040-1951\(74\)90064-X](https://doi.org/10.1016/0040-1951(74)90064-X).
- Gale, J. F. W., R. M. Reed, and J. Holder, 2007, Natural fractures in Barnett Shale and their importance for hydraulic fracture treatments: *AAPG Bulletin*, **91**, 603–622, doi: [10.1306/11010606061](https://doi.org/10.1306/11010606061).
- Gao, D., 2013, Integrating 3D seismic curvature and curvature gradient attributes for fracture characterization: Methodologies and interpretational implications: *Geophysics*, **78**, no. 2, O21–O31, doi: [10.1190/geo2012-0190.1](https://doi.org/10.1190/geo2012-0190.1).
- Gerztenkorn, A., and K. J. Marfurt, 1999, Eigenstructure-based coherence computations as an aid to 3-D structural and stratigraphic mapping: *Geophysics*, **64**, 1468–1479, doi: [10.1190/1.1444651](https://doi.org/10.1190/1.1444651).
- Gidley, J. L., 1989, Recent advances in hydraulic fracturing: SPE, Monograph Series 1, 131–146.
- Guo, Y., K. Zhang, and K. J. Marfurt, 2010, Seismic attribute illumination of Woodford Shale faults and fractures, Arkoma Basin, OK: 80th Annual International Meeting, SEG, Expanded Abstracts, 1372–1376.
- Gupta, N., 2012, Multi-scale characterization of the Woodford Shale in west-central Oklahoma: From scanning electron microscope to 3D seismic: Ph.D. thesis, University of Oklahoma.
- Harding, T. P., 1974, Petroleum traps associated with wrench fault: *AAPG Bulletin*, **58**, 1290–1304.
- Harding, T. P., 1985, Seismic characteristics and identification of negative flower structures, positive flower structures and positive structural inversion: *AAPG Bulletin*, **69**, 582–600.
- Hart, B. S., R. Pearson, and G. C. Rawling, 2002, 3-D seismic horizon-based approaches to fracture-swarm sweet spot definition in tight-gas reservoirs: *The Leading Edge*, **21**, 28–35, doi: [10.1190/1.1445844](https://doi.org/10.1190/1.1445844).
- Hennings, P. H., J. E. Olson, and L. B. Thompson, 2000, Combining outcrop data and three-dimensional structural models to characterize fractured reservoirs: An example from Wyoming: *AAPG Bulletin*, **84**, 830–849.
- Johnson, K. S., 1988, Geologic evolution of the Anadarko basin, in K. S. Johnson, ed., *Anadarko Basin Symposium*: Oklahoma Geological Survey, Circular 90, 3–12.
- Kelley, V. C., and N. J. Clinton, 1960, *Fracture systems and tectonic elements of the Colorado Plateau*: University of New Mexico Press.
- Lambert, M. W., 1993, Internal stratigraphy and organic facies of the Devonian-Mississippian Chattanooga (Woodford) Shale in Oklahoma and Kansas: Source rocks in a sequence stratigraphic framework: *AAPG Studies in Geology*, **37**, 163–176.
- Lisle, R. J., 1994, Detection of zones of abnormal strains in structures using Gaussian curvature analysis: *AAPG Bulletin*, **78**, 1811–1819.
- Marfurt, K. J., and J. Rich, 2010, Beyond curvature — Volumetric estimation of reflector rotation and convergence: 80th Annual International Meeting, SEG, Expanded Abstracts, 1467–1472.
- McClay, K., and M. Bonora, 2001, Analog models of restraining stepovers in strike-slip fault systems: *AAPG Bulletin*, **85**, 233–260.
- McLennan, J. A., P. F. Allwardt, P. H. Hennings, and H. E. Farrell, 2009, Multivariate fracture intensity prediction; Application to Oil Mountain anticline, Wyoming: *AAPG Bulletin*, **93**, 1585–1595, doi: [10.1306/07220909081](https://doi.org/10.1306/07220909081).
- Munthe, K. L., H. Omre, L. Holden, E. Damsleth, K. Heffer, T. Olsen, and J. Watterson, 1993, Subseismic faults in reservoir description and simulation: Presented at the SPE, SPE-26500-MS.
- Naylor, M. A., G. Mandl, and C. H. K. Sijpesteijn, 1986, Fault geometries in basement-induced wrench faulting under different initial stress states: *Journal of Structural Geology*, **8**, 737–752, doi: [10.1016/0191-8141\(86\)90022-2](https://doi.org/10.1016/0191-8141(86)90022-2).
- Northcutt, R. A., and J. A. Campbell, 1995, Geologic Provinces of Oklahoma: AAPG Mid-Continent Section Meeting, http://www.ogs.ou.edu/geolmapping/Geologic_Provinces_OF5-95.pdf, accessed 9 May 2016.
- Paxton, S. T., A. M. Cruse, and A. M. Krystyniak, 2006, Detailed fingerprints of global sea-level change revealed in Upper Devonian/Mississippian Woodford Shale of south-central Oklahoma: AAPG Annual Meeting, Search and Discovery Article #40211.
- Perry, W. J., 1989, Tectonic evolution of the Anadarko Basin Region, Oklahoma: U.S. Geological Survey Bulletin 1866-A.
- Reches, Z., 1976, Analysis of joints in two monoclines in Israel: *Geological Society of America Bulletin*, **87**, 1654–1662, doi: [10.1130/0016-7606\(1976\)87<1654:AOJITM>2.CO;2](https://doi.org/10.1130/0016-7606(1976)87<1654:AOJITM>2.CO;2).
- Reches, Z., 1987, Mechanical aspects of pull-apart basins and push-up swells with applications to the Dead Sea transform: *Tectonophysics*, **141**, 75–88, doi: [10.1016/0040-1951\(87\)90175-2](https://doi.org/10.1016/0040-1951(87)90175-2).
- Reches, Z., 1988, Evolution of fault patterns in clay experiments: *Tectonophysics*, **145**, 141–156, doi: [10.1016/0040-1951\(88\)90322-8](https://doi.org/10.1016/0040-1951(88)90322-8).
- Reches, Z., and A. M. Johnson, 1978, Development of monoclines: Part II. Theoretical analysis of monoclines: *Geological Society of America Memoirs*, **151**, 273–312, doi: [10.1130/MEM151-p273](https://doi.org/10.1130/MEM151-p273).
- Roberts, A., 2001, Curvature attributes and their application to 3D interpreted horizons: *First Break*, **19**, 85–100, doi: [10.1046/j.0263-5046.2001.00142.x](https://doi.org/10.1046/j.0263-5046.2001.00142.x).

- Slatt, R. M., N. Buckner, Y. Abousleiman, R. Sierra, P. R. Philp, A. Miceli-Romero, R. Portas, N. O'Brien, M. Tran, R. Davis, and T. Wawrzyniec, 2010, Outcrop/behind outcrop (quarry): Multi-scale characterization of the Woodford gas shale, Oklahoma, in J. A. Breyer, ed., *Shale reservoirs — Giant resources for the 21st century*: AAPG Memoir 97, 382–402.
- Staples, E., 2011, Subsurface and experimental analyses of fractures and curvature: M.S. thesis, University of Oklahoma.
- Staples, E., K. J. Marfurt, and Z. Reches, 2011, Curvature-fracture relations in clay experiments: 81st Annual International Meeting, SEG, Expanded Abstracts, 1908–1912.
- Sterns, D. W., 1978, Faulting and forced folding in the Rocky Mountain foreland: *Geological Society of America Memoirs*, **151**, 1–38, doi: [10.1130/MEM151](https://doi.org/10.1130/MEM151).
- Waters, G., B. Dean, R. Downie, K. Kerrihard, L. Austbo, and B. McPherson, 2009, Simultaneous hydraulic fracturing of adjacent horizontal wells in the Woodford Shale: Presented at the SPE Hydraulic Fracturing Technology Conference, doi: [10.2118/119635-MS](https://doi.org/10.2118/119635-MS).
- Wilcox, R. E., T. P. Harding, and D. R. Seely, 1973, Basic wrench tectonics: *AAPG Bulletin*, **57**, 74–96.
- Wilson, T. H., V. Smith, and A. Brown, 2015, Developing a model discrete fracture network, drilling, and enhanced oil recovery strategy in an unconventional naturally fractured reservoir using integrated field, image log, dimensional seismic data: *AAPG Bulletin*, **99**, 735–762, doi: [10.1036/10031414015](https://doi.org/10.1036/10031414015).



Zonghu Liao received a B.S. from Fuzhou University, China, and an M.S. and a Ph.D. in structural geology from the University of Oklahoma. Currently, he serves as associate professor at the China University of Petroleum, Beijing. His research interests include interpretation, structural geology, earthquakes, and landslides.



Kurt J. Marfurt began his geophysical career teaching geophysics and contributing to an industry-supported consortium on migration, inversion, and scattering (project MIDAS) at Columbia University's Henry Krumb School of Mines in New York City. In 1981, he joined Amoco's Tulsa Research Center and spent the next 18 years doing or leading research efforts in modeling, migration, signal analysis, basin analysis, seismic attribute analysis, reflection tomography, seismic inversion, and multicomponent data analysis. In 1999, he joined the University of Houston as a professor in the Department of Geosciences and as a director of the Allied Geophysics Laboratories. He is a member of the Geophysical Societies of Tulsa and Houston, SEG, EAGE, AAPG, AGU, and SIAM, and he serves as an assistant editor for *GEOPHYSICS*. His current research activity includes prestack imaging, velocity analysis and inversion of converted waves, computer-assisted pattern recognition of geologic features on 3D seismic data, and interpreter-driven seismic processing. His research interests include seismic signal analysis, 3D seismic attributes, seismic velocity analysis, subsurface imaging, and multicomponent data analysis.



Ze'ev Reches received a B.S. and an M.S. in geology from Hebrew University, Israel, and a Ph.D. in structural geology from Stanford University. He serves as professor of structural geology at the University of Oklahoma. His prior work includes positions at Arizona State University, Stanford University, and the U.S. Geological Survey at Menlo Park, California, and Hebrew University, Israel. His research interests include earthquake and fault processes and rock mechanics.

Biographies and photographs of the other authors are not available.